5-15-1969

Lattice Dynamics of NaF

Arnold Karo
University of California, Livermore, California

John R. Hardy
University of Nebraska - Lincoln

Lattice Dynamics of NaF*

ARNOLD M. KARO
Lawrence Radiation Laboratory, University of California, Livermore, California 94550

AND

JOHN R. HARDY
Behlen Laboratory of Physics, University of Nebraska, Lincoln, Nebraska 68508

(Received 25 July 1968)

The results of an extended calculation of the normal modes of the NaF lattice are presented. Three models have been considered: a "rigid-ion" (RI) model, a "deformation-dipole" model with central F^--F^- short-range interactions (DDNNN), and a "deformation-dipole" model including both central F^--F^- interactions and a noncentral component in the first-neighbor, short-range interactions [DDNNN(NC)]. For each of these models we have derived frequency spectra for both 300 and 0°K input parameters, the associated dispersion curves for symmetry directions, Debye characteristic temperatures Θ_D, moment functions $\omega_D(n)$, and the Na^+ and F^- Debye-Waller parameters B_1 and B_2 and their ratio B_1/B_2. Of the three models, the two DD variations give good agreement with the observed dispersion curves, the DDNNN models being slightly better and giving somewhat closer agreement with the observed B values.

I. INTRODUCTION

SOME time ago we presented the results of a systematic investigation into the lattice dynamics of most of the NaCl-structure alkali halides.[1] This work was based on the "deformation-dipole" (DD) model, originally developed for NaCl.[2] This model is superior to the old "rigid-ion" (RI) model of Kellermann[3] in that it takes into account the fact that the ions are not rigid but can be polarized both by the electric field associated with a lattice wave and by the associated changes in the short-range repulsive interaction between the ions.

One of the input parameters used in the earlier work on NaF was the Szigeti effective charge[4] e^* for which we took the value $0.93e$ (e=the magnitude of the electronic charge) from Born and Huang.[5] Subsequent experimental work by Lowndes[6] has revealed that this value is seriously in error, and that the revised value is $0.83e$. In a paper that followed this early work,[7] we presented a much more detailed treatment of NaCl in which a precise vibrational frequency spectrum for this crystal was derived, together with equally precise phonon-dispersion curves for all the principal symmetry directions. Because the earlier work on NaF was based on a poor estimate of e^*, it is both desirable to repeat it with a more accurate value and at the same time to make a detailed investigation of the lattice dynamics, similar to the work on NaCl. This work has also been stimulated by the recent measurements[8] of the (100), (110), and (111) phonon-dispersion curves of NaF which, as we shall see, are in good agreement with the revised theoretical calculations. Finally, it is highly desirable, from the point of view of work on phonon-assisted optical transitions at defect centers in NaF, that there should be available a reliable lattice vibrational frequency spectrum.

II. DESCRIPTION OF MODEL

The ultimate object of theoretical calculations on the frequency versus wave-vector dispersion relations for phonons in any given material is to develop a means of *predicting* these relations from first principles. Such a theory will contain no disposable parameters. At present it does not seem practicable to develop such a theory, and some intermediate stage is necessary as a first step. This is offered by both the DD model and the simple "shell model,"[9] each of which attempts to predict the dispersion curves on the basis of a potential function containing few enough parameters to be fixed from the elastic and dielectric constants. Moreover, the various parameters all have a clearly defined physical significance. In this way it has been shown[1,9] that one can obtain a much better fit to the measured dispersion curves than is provided by the RI model. This test has been applied, for example, in the cases of NaI [9] and KBr.[10] However, the resulting agreement is not perfect, and the shell model has been extended[10] in such a way that the number of disposable parameters is much increased. These are then determined by least-squares fitting to the observed dispersion curves, and an even better fit to the experimental data is obtained. Recently, Nusimovici and Birman[11] have questioned the useful-

* Work performed in part under the auspices of the U. S. Atomic Energy Commission.

[1] A. M. Karo and J. R. Hardy, Phys. Rev. **129**, 2024 (1963).
[2] J. R. Hardy, Phil. Mag. **4**, 1278 (1959).
[3] E. W. Kellermann, Phil. Trans. Roy. Soc. London **238**, 513 (1940); Proc. Roy. Soc. (London) **A178**, 17 (1941).
[4] B. Szigeti, Proc. Roy. Soc. (London) **A204**, 51 (1950).
[5] M. Born and K. Huang, in *Dynamical Theory of Crystal Lattices* (Oxford University Press, New York, 1954), p. 85.
[6] R. Lowndes, Phys. Letters **21**, 26 (1966).
[7] A. M. Karo and J. R. Hardy, Phys. Rev. **141**, 696 (1966).
[8] W. J. L. Buyers, Phys. Rev. **153**, 923 (1967).
[9] A. D. B. Woods, W. Cochran, and B. N. Brockhouse, Phys. Rev. **119**, 980 (1960).
[10] R. A. Cowley, W. Cochran, B. N. Brockhouse, and A. D. B. Woods, Phys. Rev. **131**, 1030 (1963).
[11] M. A. Nusimovici and J. L. Birman, Phys. Rev. **156**, 925 (1967).

ness of this procedure since it very rapidly leads to a theory containing even more disposable parameters than the old Born–von Karman[12] approach based on interatomic force constants. From a practical point of view, this seems to be a valid objection. Also, given two models each containing the same number of disposable parameters, it would appear hard to justify the claim that one is more fundamental than the other. Certainly, it does not seem very logical to defend the simple shell model on the grounds that it reduces the number of disposable parameters to a minimum, *vis-à-vis* a force-constant model, and then to justify the extended shell model on the grounds that it effectively maximizes the number of disposable parameters. This appears to be effectively what one is doing by allowing as many input parameters as possible to "float" in a least-squares fit to the experimental data. It would seem to be far more reasonable to argue that the extended shell model is only a good interpolation scheme which is useful *because* it contains so many disposable parameters and thereby maximizes the amount of experimental information that goes into the calculation of phonon frequencies at a general point in the reduced zone.

In the present paper we shall be describing calculations based on the DD model described in detail in an earlier paper[13] in which all the parameters have a clear physical meaning. Our object is to see how well we can *predict* the observed dispersion curves, keeping the number of parameters down to the minimum necessary to fit the observed dielectric and elastic constants.

To demonstrate the effects of polarization corrections, a set of "reference" calculations based on the RI model have been carried through, and these results will also be presented. In the RI calculations the ions are assumed to displace as rigid spheres of charge $\pm e$, where e is the magnitude of the electronic charge, with the crystal kept in equilibrium by a short-range central repulsion acting only between first neighbors. Given these assumptions, the dynamical matrix can be constructed using only the observed lattice constant and the compressibility. In the DD calculations, the short-range part of the dynamical matrix has been modified to include next-nearest-neighbor interactions between the F^- ions, and this variation is referred to as the DDNNN model. Using this model, one can fit both the observed infrared dispersion frequency ω_0 and the shear modulus C_{44} which, between them, effectively determine the first and second derivatives of the F^--F^- interaction.

As in our earlier work,[2,7,13] both the positive and negative ions are assumed to acquire dipole moments given by the products of their self-consistent TKS[14] polarizabilities and the effective fields at their centers. In addition, the F^- ions are assumed to acquire additional dipole moments, the "deformation" dipole moments, which experience the effective fields at the F^- ion centers and are determined by their nearest-neighbor configurations and the observed value of e^*, the Szigeti effective charge.[4] In this way, we fit the high- and low-frequency dielectric constants ϵ_∞ and ϵ_0, ω_0, the compressibility β, and C_{44}. To fit C_{11} and C_{12} separately, we can introduce a noncentral component into the nearest-neighbor interaction,[9] and results for this DDNNN(NC) model will also be presented.

III. DETAILS OF CALCULATIONS

In this paper we are concerned with the calculation of what may be described as "single-phonon" data, i.e., with properties that depend directly on the frequency distribution of the plane-wave normal modes of the NaF lattice. A complementary account of calculations of certain "two-phonon" properties of the lattice, i.e., the second-order Raman effect, has been given in another paper.[15] In the present paper, calculations for the normal-mode frequency distribution, the specific heats, and the Debye-Waller factors for both Na^+ and F^- are described. For each model except the DDNNN model, the calculation of these properties is carried out by first deriving the plane-wave normal-mode eigenfrequencies and eigenvectors for a sample of 8000 wave vectors ($\mathbf{q}$ vectors) within the first Brillouin zone. Such a sample is adequate for calculating these quantities, but is not sufficient to define the finer details of the frequency spectrum if one uses the standard histogram technique. To improve matters in this respect, we have counted the calculated frequencies into very narrow sample intervals and smoothed the resulting "noisy" histogram by fitting Gaussians to each step, the heights of the Gaussians chosen to be equal to the steps and with a common half-width adjusted to obtain the best smoothing consistent with retaining genuine structure. For the DDNNN model, samples of 64 000 $\mathbf{q}$ vectors have been used and the results combined with the Gaussian smoothing technique. On the basis of earlier work on NaCl,[7] this would appear to define the true frequency spectra with good precision. Calculations of the frequency distributions can be supplemented by plotting on the same figure, using a common frequency scale, the corresponding ω-versus-$\mathbf{q}$ dispersion curves for the principal symmetry directions, thereby locating the van Hove[16] singularities in $N(\omega)$.

The specific heats are calculated at constant volume, or, more precisely, at fixed volume. Values of the input parameters, in particular the lattice constant, are those appropriate either to 0 or 300°K. The specific heats are then obtained over the whole range of temperatures from 0 to 300°K, using first one set and then the other

[12] M. Born and Th. von Karman, Z. Physik **13**, 297 (1912).
[13] J. R. Hardy, Phil. Mag. **7**, 315 (1962).
[14] J. R. Tessman, A. H. Kahn, and W. Shockley, Phys. Rev. **92**, 890 (1953).
[15] J. R. Hardy, A. M. Karo, I. W. Morrison, C. T. Sennett, and J. P. Russell, Phys. Rev. **179**, 837 (1969).
[16] L. van Hove, Phys. Rev. **89**, 1189 (1953).

TABLE I. Input parameters for NaF calculations.

Model	Temperature (°K)	Lattice constant $r_0(10^{-8}$ cm)	Compressibility $\beta(10^{-12}$ cm²/dyn)	Screening radius $\rho(10^{-8}$ cm)	Effective charge e^*/e	Dielectric constants ϵ_0	ϵ_∞	Infrared disp. frequency $\omega_0(10^{13}$ sec$^{-1})$	Ionic polarizabilities $\alpha_+(10^{-24}$ cm³)	$\alpha_-(10^{-24}$ cm³)	Elastic constants C_{44} $(10^{11}$ dyn/cm²)	C_{12} $(10^{11}$ dyn/cm²)
RI	0	2.2967	1.8210	...	...	...	...	...	...	...	...	...
	300	2.3100	2.0590	...	...	...	...	...	...	...	...	...
DDNNN	0	2.2967	1.8210	0.2603	0.8374	4.809	1.6377	4.7465	0.255	0.759	3.0358	...
	300	2.3100	2.0590	0.2826	0.8270	5.100	1.7392	4.6400	0.255	0.759	2.800	...
DDNNN(NC)	0	2.2967	1.8210	0.2603	0.8374	4.809	1.6377	4.7465	0.255	0.759	3.0358	2.5854
	300	2.3100	2.0590	0.2826	0.8270	5.100	1.7392	4.6400	0.255	0.759	2.800	2.4300

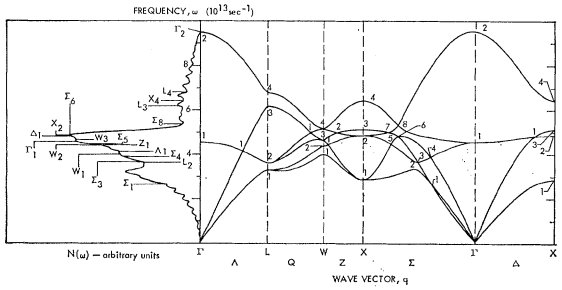

(a)

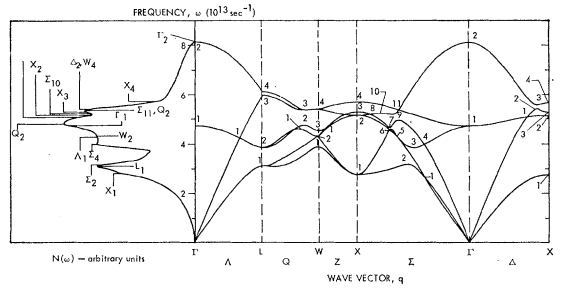

(b)

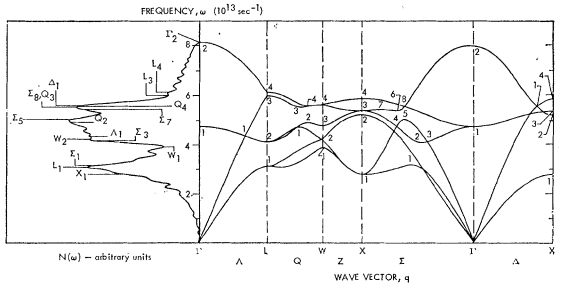

(c)

FIG. 1. Combined frequency spectra and dispersion curves for the three models described in the text with 0°K input parameters. The c.p.'s along each symmetry axis and at each symmetry point are labeled 1, 2, etc., in order of increasing frequency. On the spectrum itself corresponding c.p.'s that can be associated with the more prominent features of the spectrum are labeled according to the notation of the symmetry axis or point, with a subscript indicating the relative position along the frequency axis of the c. p. Thus Λ_1 means the lowest-frequency c.p. along the Λ direction. A more complete analysis is given in University of California, Livermore Report UCRL-71085, 1968 (unpublished). (a) The RI model, sample of 8000 **q** vectors; (b) the DDNNN model, sample of 64 000 **q** vectors; and (c) the DDNNN(NC) model, sample of 8000 **q** vectors.

set of parameters. In practice, one is more likely to be concerned with the low-temperature specific heats obtained from 0°K input parameters. From the calculated specific heats, values are derived for the effective Debye temperature $\Theta_D(T)$ as a function of temperature T.

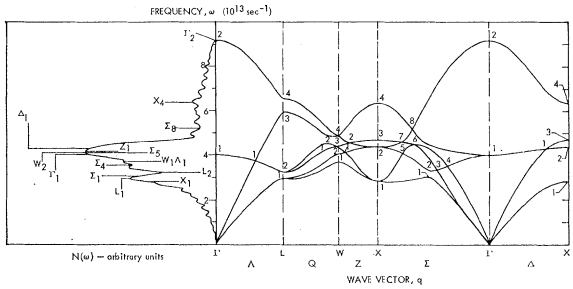

(a)

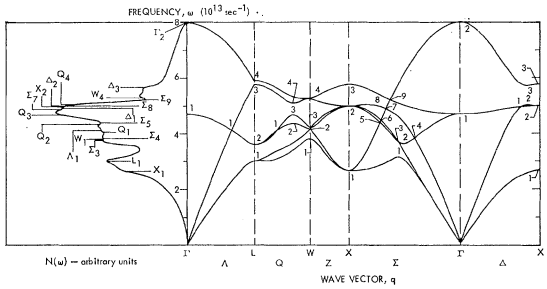

(b)

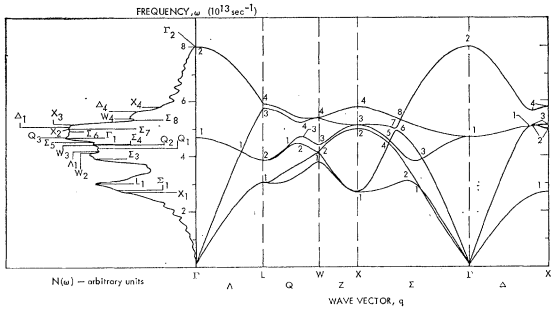

(c)

FIG. 2. Results as for Fig. 1 with input parameters appropriate to 300°K. (a) The RI model, sample of 8000 **q** vectors; (b) the DDNNN model, sample of 64 000 **q** vectors; and (c) the DDNNN(NC) model, sample of 8000 **q** vectors.

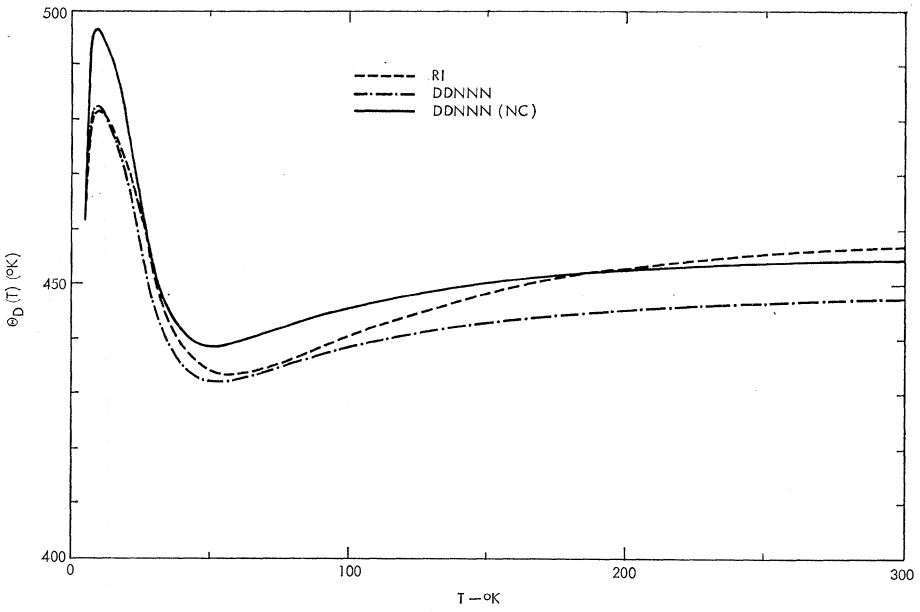

FIG. 3. Plots of the characteristic Debye temperature $\Theta_D(T)$ against temperature for the three models, with 0°K input parameters. The falloff of the curves as $T \rightarrow 0$ is characteristic of inadequate sampling as $\mathbf{q} \rightarrow 0$ and has no other significance.

This function was first introduced by Blackman[17] and is obtained by fitting a Debye specific-heat function to the calculated specific heat, using Θ_D as a disposable parameter. Finally, one may also derive the moment function $\omega_D(n)$, originally introduced by Barron *et al.*,[18] defined by the equation

$$\omega_D(n)=[\tfrac{1}{3}(n+3)\mu_n]^{1/n},$$

where μ_n is the nth moment of the frequency distribution. The advantage of using either $\Theta_D(T)$ or $\omega_D(n)$ is that they are proportionately much more sensitive to the details of $N(\omega)$ than the specific heat.

Unfortunately, there do not appear to be available any experimental results with which one can compare the theoretical specific-heat data, but we hope that the present paper will encourage such work.

IV. DISPERSION CURVES, FREQUENCY SPECTRA, AND SPECIFIC-HEAT DATA

In Figs. 1 and 2 we present the frequency spectra and dispersion curves for the three models, RI, DDNNN, and DDNNN(NC). Figure 1 shows the results for 0°K input (see Table I), and Fig. 2 shows the corresponding data for the 300°K [room temperature (RT)] parameters of Table I. On all six spectra are shown the positions of the various van Hove[16] critical points (c.p.) implied by maxima, minima, or crossovers in the calculated dispersion curves. Both sets of curves are shown since there is a marked differential shift in the various branches of the frequency spectrum for both NNN models as one changes the input parameters from RT to 0°K values. As can readily be seen, this results in quite significant changes in the forms of the spectra. Although much of the fine structure in the spectra for the RI and DDNNN(NC) models is due to the small sample, there is a large amount of structure in the calculated spectra that is clearly genuine since the various features can be correlated with c.p.'s on the dispersion curves. It can also be seen that some c.p.'s are not evident in the frequency spectra; finer sampling might reveal these, but they are probably very weak. In Figs. 3 and 4 we plot the calculated $\Theta_D(T)$ and $\omega_D(n)$ curves for each of the models, and since experimental results would be most appropriate for the frequency spectrum at 0°K, only the results for 0°K input are shown. It can be seen that there are significant differences between the three sets of results, and the corresponding experimental data should clearly favor one of the three models. This sort of comparison is still of interest even when experimental dispersion curves

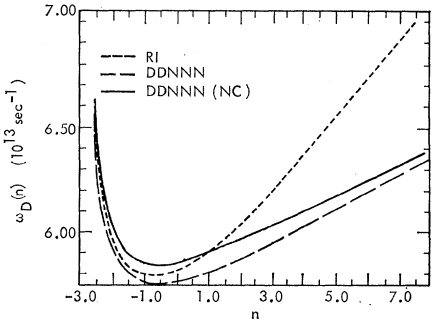

FIG. 4. Plots of the moment function $\omega_D(n)=[\frac{1}{3}(n+3)\mu_n]^{1/n}$, where μ_n is the nth moment of the frequency spectrum, against n for the three models, with 0°K input parameters.

[17] M. Blackman, in *Reports on Progress in Physics* (The Physical Society of London, 1941), Vol. 8, p. 11.

[18] T. H. K. Barron, W. T. Berg, and J. A. Morrison, Proc. Roy. Soc. (London) **A242**, 478 (1957).

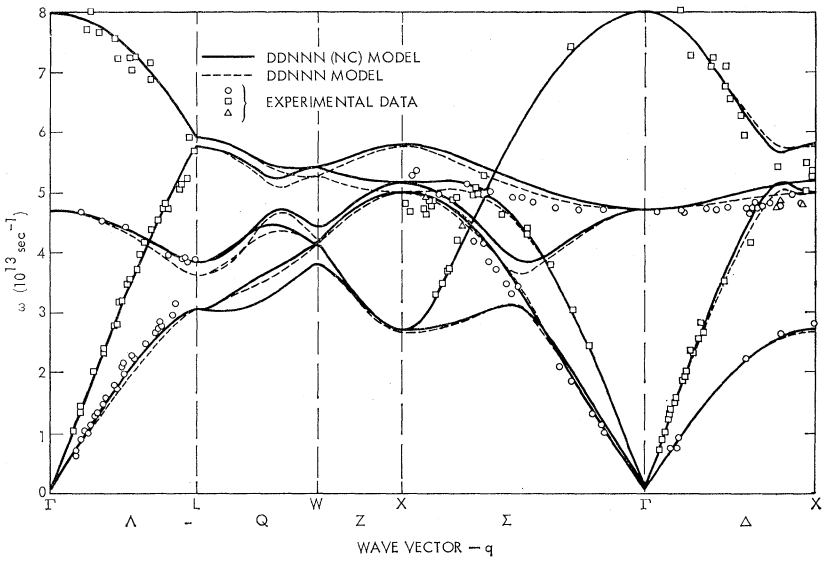

FIG. 5. Comparison of the calculated dispersion curves for both the DDNNN and DDNNN(NC) models (300°K input data) with the experimental data of Buyers (Ref. 8).

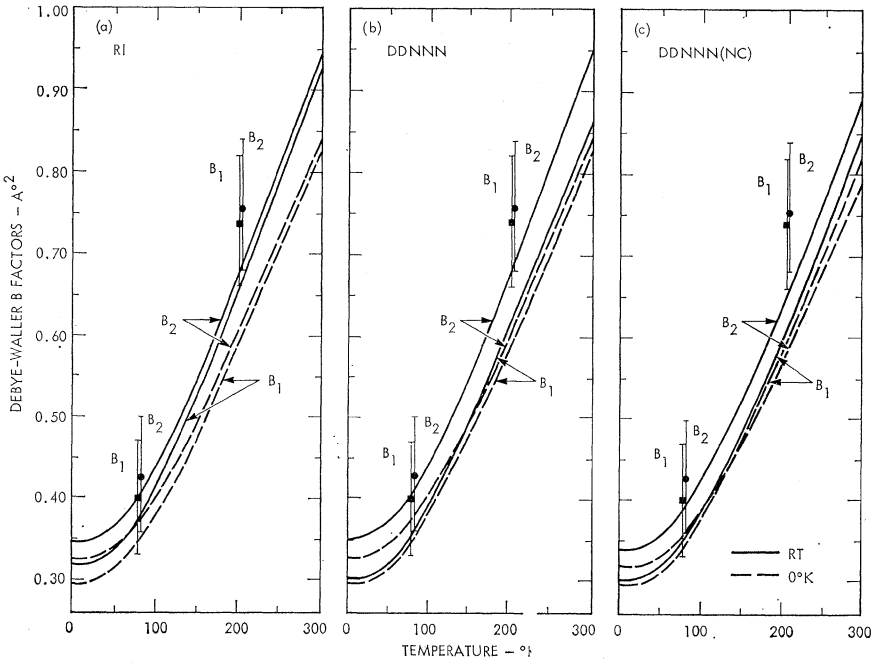

FIG. 6. Plots of the Debye-Waller coefficients B_1 and B_2 against temperature for the three models, using both 0 and 300°K input parameters. The experimental values (Ref. 20) are also shown. B_2 values have been shifted slightly on the temperature scale so that the experimental inaccuracy can be shown by error bars. (a) The RI model, sample of 8000 **q** vectors; (b) the DDNNN model, sample of 64 000 **q** vectors; and (c) the DDNNN(NC) model, sample of 8000 **q** vectors.

are available, since the specific-heat data are to some extent sensitive to the whole frequency spectrum and thus to the accuracy to which the theoretical model reproduces the frequencies at all points within the reduced zone and not merely those lying along high-symmetry directions.

The dispersion curves are replotted in Fig. 5, together with the results of recent measurements of the phonon-dispersion curves.[8] The present DD models reproduce the observed frequencies significantly better than the simple shell model.[8] One possible reason for this is that we allow for the polarizability of the positive ion, which, as can be seen from Table I, is of the same order of magnitude as that of the F^- ion. Consequently, it is probable that assigning the whole polarizability to the F^- ion as is done in the simple shell-model calculation could produce a significant change for the worse.[19]

[19] We have included NNN interactions in our calculations while these are omitted from the simple shell model. However, we have also carried through DD calculations in which these interactions are neglected and find the results to be so close to our present data that we have not included them in the present paper. Thus, it would appear that the improved fit is due almost entirely to the differences between the dipolar parts of the shell model and the DD-model dynamical matrices.

Moreover, it can be seen that both NNN models give results about equally close to the experimental curves, even though the 0°K versions of these models lead to different Θ_D and $\omega_D(n)$ curves. This gives added weight to the point made earlier that the measured phonon-dispersion curves for three high-symmetry directions do not define the dynamical matrix completely and that the comparison of theoretical and experimental specific-heat data is a useful complementary test for any model, even though the model might provide a good description of the dispersion curves alone.

Our complementary investigation of the second-order Raman spectra of NaF[15] is based on the DDNNN model. It is probable that this model is slightly better for this purpose, and for this reason it has been chosen for the most detailed investigation in the present paper.

V. DEBYE-WALLER FACTORS

Thus far, all the "single-phonon" properties that we have been considering depend only on the normal-mode eigenfrequencies. It is of considerable interest to find similar quantities which also depend on the eigenvector. To this end we have computed the thermal mean-square displacements of both the Na^+ and the F^- ions as functions of temperature. These are experimentally measured in determinations of the Debye-Waller factors for the two types of ions, which give B_1 and B_2 (in the conventional notation), where

$$B_{1,2}=(8\pi^2/3)\langle U_{1,2}^2(0)\rangle_T,$$

$U_{1,2}(0)$ being the magnitude of the displacement of atom 1 or 2, $1\equiv+$, $2\equiv-$, in the zeroth unit cell, and $\langle\ \rangle_T$ indicating the thermal average value. Thus,

$$B_{1,2}=\frac{8\pi^2}{3}\frac{1}{N}\sum_{\mathbf{q}}\sum_{j}\frac{m_j(\mathbf{q})\hbar\{\bar{n}[\omega_j(\mathbf{q})]+\frac{1}{2}\}}{M_{1,2}\omega_j(\mathbf{q})}\sum_{\alpha}|\sigma_j^{1,2}{}_{\alpha}(q)|^2,$$

where N is the number of sample $\mathbf{q}$ vectors within the first zone, j is the branch index, $\omega_j(\mathbf{q})$ is the angular frequency of the jth branch at wave vector $\mathbf{q}$, $n[\omega_j(\mathbf{q})]$ is the thermal occupation number of this mode, $\sigma_j^{1,2}{}_{\alpha}(\mathbf{q})$ is the α component of the positive- (1) or negative- (2) ion component of the corresponding eigenvector, $M_{1,2}$ are the appropriate ion masses, and $m_j(\mathbf{q})$ is the weighting factor for the point being considered in the Brillouin zone. The computed results for B_1, B_2, and B_1/B_2 for the three models are shown in Figs. 6 and 7. In each case curves are shown for both RT and 0°K input parameters. On the same curves we also show

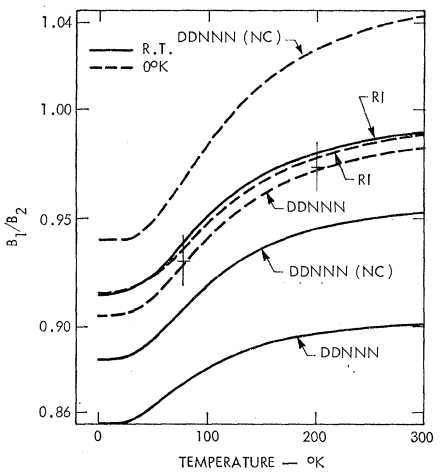

FIG. 7. Plots of the ratios B_1/B_2 for the three models, using both 0 and 300°K input parameters for each case.

the recently measured values of B_1 and B_2, which refer to 78 and 202°K.[20] It is evident that for B_1 and B_2 separately the DDNNN model with RT input gives good agreement with experiment, although B_1 is too low. However, too much weight should not be given to this comparison since the experimental values measured using x rays are somewhat uncertain, and also it is quite possible that anharmonic corrections[21] are significant at the higher temperature. It can be seen from Fig. 7 that the ratio B_1/B_2 is very sensitive to the models used, and we would suggest that measurements of this ratio as a function of temperature are probably the best means of distinguishing between the various models.

Finally, it should be noted that the calculated B values at intermediate temperatures (i.e., $T\sim$the average Θ_D) are about equally sensitive to both the eigenfrequencies and the eigenvectors of all the normal modes. This makes the comparison between calculated and observed B values a significantly better test of the theoretical models than specific-heat data.

ACKNOWLEDGMENT

The authors would like to express their gratitude to Ira Morrison of the Computation Division of the University of California Lawrence Radiation Laboratory for designing and carrying out the computational part of this investigation.

[20] M. Merisalo, Ann. Acad. Sci. Fennicae **245**, 1 (1967).
[21] R. A. Cowley, Advan. Phys. **13**, 423 (1963).